MOLECULAR AND CELLULAR BIOLOGY, Aug. 1995, p. 3998–4008 Vol. 15, No. 8
0270-7306/95/$04.00+0

The Essential Helicase Gene *RAD3* Suppresses Short-Sequence Recombination in *Saccharomyces cerevisiae*

ADAM M. BAILIS,* SILVINA MAINES, AND M. TINA NEGRITTO

Department of Molecular Genetics of the Beckman Research Institute and Division of Gene Therapy, City of Hope National Medical Center, Duarte, California 91010

Received 18 November 1994/Returned for modification 12 January 1995/Accepted 28 April 1995

We have isolated an allele of the essential DNA repair and transcription gene *RAD3* that relaxes the restriction against recombination between short DNA sequences in *Saccharomyces cerevisiae*. Double-strand break repair and gene replacement events requiring recombination between short identical or mismatched sequences were stimulated in the *rad3-G595R* mutant cells. We also observed an increase in the physical stability of double-strand breaks in the *rad3-G595R* mutant cells. These results suggest that the *RAD3* gene suppresses recombination involving short homologous sequences by promoting the degradation of the ends of broken DNA molecules.

All organisms must repair the damage to their DNA that results from environmental stress and normal metabolism. Genetic recombination is one of several pathways that have evolved to repair this damage (13). This mode of repair can lead to deleterious consequences, however, because recombination between dispersed duplicate (ectopic) sequences can result in genome rearrangements or gene inactivation or both (42). These events are also implicated in human disease (20, 24). Both DNA sequence length (2, 26, 51, 53, 58) and identity (6, 18, 36, 43, 45, 47) are important determinants of the rate of recombination between repeated DNA sequences. What remains largely unclear is how short sequence length and mismatching hinder recombination. We took a genetic approach to studying the control of ectopic recombination in *Saccharomyces cerevisiae*. In a search for mutants that stimulate this recombination, we isolated an allele of the *RAD3* gene (*rad3-G595R*) that increased the rate of recombination between sequences that share short lengths of perfect or imperfect homology.

The *RAD3* gene encodes a helicase (61) that is an essential component of the transcription and DNA repair complex TFIIH (factor B [10, 66]) and is highly homologous to the human nucleotide excision repair gene *XPD* (60, 67). Many *rad3* mutants have been isolated (13). These mutants exhibit a wide array of overlapping phenotypes including altered transcription (16), DNA repair (40, 48, 72), and recombination (37). One set of mutants, originally designated *rem*, were identified on the basis of their mutator and hyperrecombination phenotypes (14). The *rem* genes were subsequently found to be alleles of *RAD3* and are thought to lead to the creation of recombinogenic double-strand breaks (37). Another mutant allele, *rad3-2*, is not hyperrecombinant but does decrease gene conversion tract length during intrachromosomal recombination (1). These diverse recombination phenotypes may be due to defects in the transcription of important recombination genes or to direct effects of mutant Rad3 proteins on recombination.

White and Haber (71) analyzed the repair of double-strand breaks in DNA by homologous recombination between unlinked, duplicate sequences at the molecular level and showed that double-strand breaks are subject to extensive 5′-end degradation in wild-type cells. This processing is thought to be crucial for producing a single-stranded 3′ end (3, 7, 59, 71) that can invade the recombination partner and form heteroduplex DNA, an essential recombination intermediate (22, 34, 46, 62). If degradation of the ends is too extensive, however, enough homology with the unlinked recombination partner can be removed that the broken sequence may no longer be efficiently healed by recombination with that partner. In this study, we found that an increase in the stability of the ends of double-strand breaks in *rad3-G595R* mutant cells is associated with a stimulation of recombination between short homologous sequences, suggesting that the *RAD3* gene may restrict recombination by directly or indirectly facilitating exonucleolytic degradation of the ends of broken molecules. On the basis of our results from the genetic and physical analysis of recombination in *rad3-G595R* mutant cells, we propose models for how *RAD3* may be acting to discourage ectopic recombination, thereby contributing to genome stability.

MATERIALS AND METHODS

Strains. All yeast strains used in this study were isogenic derivatives of W303-1A or W303-1B (63) and are listed in Table 1. Standard methods were used for strain construction, growth, and maintenance (54). Both spheroplast formation (19) and alkali cation (23) methods for transforming yeast cells were used.

Plasmids. All important plasmid constructions are listed in Table 2. Standard molecular biological methods were used throughout their construction.

Mutagenesis and screening for temperature-sensitive hyperrecombination mutants. Wild-type cells (carrying mismatched assay 1 [Fig. 1]) were mutagenized to 20 to 40% viability with ethyl methanesulfonate according to an established protocol (54). Approximately 100,000 mutagenized cells were screened for the inability to grow at 37°C. Temperature-sensitive (Ts) colonies were then assayed for altered double-strand break-stimulated recombination by a patch assay, as follows. The Ts colonies were streaked into 2-cm^2 squares on nonselective medium (without Trp but with *S*-adenosylmethionine [AdoMet]) and incubated at 30°C for 5 days. The patches were then replica plated onto medium that induces double-strand break formation and selects for recombinants (without Trp or AdoMet but with galactose) and incubated at 30°C for 5 days. Patches of wild-type cells had zero to four $AdoMet^+$ recombinant papillae at the end of 5 days. Of 235 Ts mutants, 3 consistently had 10 or more $AdoMet^+$ recombinant papillae in a 2-cm^2 patch. The mutant that had the highest level of recombination was selected for further study.

Mapping and sequencing of the *rad3* allele. A 4.0-kb *Mlu*I-*Sal*I DNA fragment containing the *RAD3* gene was cloned into the yeast centromere plasmid pRS416 (8) that contains the yeast *URA3* gene and was digested with several restriction

* Corresponding author. Mailing address: Department of Molecular Genetics of the Beckman Research Institute and Division of Gene Therapy, City of Hope National Medical Center, 1450 E. Duarte Rd., Duarte, CA 91010. Phone: (818) 359-8111, ext. 4031. Fax: (818) 301-8271. Electronic mail address: abailis@bricoh.coh.org.

TABLE 1. *S. cerevisiae* strains used in this study[a]

Strain	Genotype
W1019-3A	*MAT*::*LEU2 ade2-1 can1-100 leu2-3,112 trp1-1 ura3-1 sam1*-Δ*Bgl*II-*HOcs sam2*::*HIS3 HIS3*::*sam2*-Δ*Sal*I pGHOT (*GAL*::*HO*, *TRP1*)
W1136-2C	*MAT*::*LEU2 ade2-1 can1-100 leu2-3,112 trp1-1 ura3-1 sam1*-Δ*Bgl*II-*HOcs sam2*::*HIS3 HIS3*::*sam2*-Δ*Sal*I *rad3-G595R* pGHOT(*GAL*::*HO*, *TRP1*)
U780	*MAT*::*LEU2 ade2-1 can1-100 leu2-3,112 trp1-1 ura3-1 sam1*-Δ*Bgl*II-*HOcs sam2*::*HIS3 HIS3*::*sam2*-Δ*Sal*I::*URA3*::*SAM2* pGHOT (*GAL*::*HO*, *TRP1*)
U781	*MAT*::*LEU2 ade2-1 can1-100 leu2-3,112 trp1-1 ura3-1 sam1*-Δ*Bgl*II-*HOcs sam2*::*HIS3 HIS3*::*sam2*-Δ*Sal*I *pms1*::*LEU2* pGHOT (*GAL*::*HO*, *TRP1*)
U797	*MAT*α *ade2-1 can1-100 leu2-3,112 trp1-1 ura3-1 sam1*-Δ*Bgl*II-*HOcs sam2*::*HIS3 HIS3*::*sam2*-Δ*Sal*I *rad3-G595R* pGHOT (*GAL*::*HO*, *TRP1*)
U807	*MAT*::*LEU2 ade2-1 can1-100 leu2-3,112 trp1-1 ura3-1 SAM1 sam2*::*HIS3 HIS3*::*sam2*-Δ*Sal*I *rad3-G595R* pGHOT (*GAL*::*HO*, *TRP1*), pJM3 (*MAT***a**, *URA3*)
U834	*MAT*::*LEU2 ade2-1 can1-100 leu2-3,112 trp1-1 ura3-1 sam1*-Δ*Bgl*II-*HOcs sam2*::*HIS3 HIS3*::*sam2*-Δ*Sal*I::*URA3*::*SAM2 rad3-G595R* pGHOT (*GAL*::*HO*, *TRP1*)
ABT79	*MAT*::*LEU2 ade2-1 can1-100 leu2-3,112 trp1-1 ura3-1 sam1*-Δ*Bgl*II-*HOcs sam2*::*HIS3 HIS3*::*sam2*-Δ*Sal*I *rad3-G595R* pGHOT (*GAL*::*HO*, *TRP1*), pRS416
ABT80	*MAT*::*LEU2 ade2-1 can1-100 leu2-3,112 trp1-1 ura3-1 sam1*-Δ*Bgl*II-*HOcs sam2*::*HIS3 HIS3*::*sam2*-Δ*Sal*I *rad3-G595R* pGHOT (*GAL*::*HO*, *TRP1*), pRS416-*RAD3*
W1159-20D	*MAT*::*LEU2 ade2-1 can1-100 leu2-3,112 trp1-1 ura3-1 sam1*::*LEU2 sam2*-Δ*Eco*RV-*HOcs HIS3*::*sam1*-Δ*Sal*I, pGHOT (*GAL*::*HO*, *TRP1*)
U852	*MAT*::*LEU2 ade2-1 can1-100 leu2-3,112 trp1-1 ura3-1 sam1*::*LEU2 sam2*-Δ*Eco*RV-*HOcs HIS3*::*sam1*-Δ*Sal*I *rad3-G595R* pGHOT (*GAL*::*HO*, *TRP1*)
W1222-1C	*MAT*α *ade2-1 can1-100 his3-11,15 leu2-3,112*, *ura3-1*, *rad3-G595R*
U856	*MAT*::*LEU2 ade2-1 can1-100 leu2-3,112 trp1-1 ura3-1 sam1*-Δ*Bgl*II *sam2*::*HIS3 HIS3*::*sam2*-Δ*Sal*I-*HOcs* pGHOT (*GAL*::*HO*, *TRP1*)
U860	*MAT*::*LEU2 ade2-1 can1-100 leu2-3,112 trp1-1 ura3-1 sam1*-Δ*Bgl*II *sam2*::*HIS3 HIS3*::*sam2*-Δ*Sal*I-*HOcs rad3-G595R* pGHOT (*GAL*::*HO*, *TRP1*)
U857	*MAT*::*LEU2 ade2-1 can1-100 leu2-3,112 trp1-1 ura3-1 sam1*-Δ*Bgl*II-*HOcs sam2*::*HIS3 HIS3*::*sam1*-Δ*Sal*I pGHOT (*GAL*::*HO*, *TRP1*)
U858	*MAT*::*LEU2 ade2-1 can1-100 leu2-3,112 trp1-1 ura3-1 sam1*-Δ*Bgl*II-*HOcs sam2*::*HIS3 HIS3*::*sam1*-Δ*Sal*I *rad3-G595R* pGHOT (*GAL*::*HO*, *TRP1*)
ABX66	*MAT***a**/*MAT*α *ade2-1*/*ade2-1 can1-100*/*can1-100 leu2-3,112*/*leu2-3,112 his3-11,15*/*his3-11,15 trp1-1*/*trp1-1 ura3-1*/*ura3-1 SAM1*/*sam1*::*LEU2 sam2*::*HIS3*/*sam2*::*HIS3 rad3-G595R*/*rad3-G595R*
ABX67	*MAT***a**/*MAT*α *ade2-1*/*ade2-1 can1-100*/*can1-100 leu2-3,112*/*leu2-3,112 his3-11,15*/*his3-11,15 trp1-1*/*trp1-1 ura3-1*/*ura3-1 SAM1*/*sam1*::*LEU2 sam2*::*HIS3*/*sam2*::*HIS3*
ABX73	*MAT***a**/*MAT*α *ade2-1*/*ade2-1 can1-100*/*can1-100 leu2-3,112*/*leu2-3,112 his3-11,15*/*his3-11,15 trp1-1*/*trp1-1 ura3-1*/*ura3-1 SAM1*/*sam1*::*LEU2 sam2*::*HIS3*/*sam2*::*HIS3 SSL1-3*/*SSL1-3*
ABX74-6C	*MAT*::*LEU2 ade2-1 can1-100 leu2-3,112 trp1-1 ura3-1 sam1*-Δ*Bgl*II-*HOcs sam2*::*HIS3 HIS3*::*sam1*-Δ*5′*, Δ*Sal*I, pGHOT (*GAL*::*HO*, *TRP1*)
ABX74-17B	*MAT*::*LEU2 ade2-1 can1-100 leu2-3,112 trp1-1 ura3-1 sam1*-Δ*Bgl*II-*HOcs sam2*::*HIS3 HIS3*::*sam1*-Δ*5′*, Δ*Sal*I, *rad3-G595R* pGHOT (*GAL*::*HO*, *TRP1*)
ABT98	*MAT*::*LEU2 ade2-1 can1-100 leu2-3,112 trp1-1 ura3-1 sam1*-Δ*Bgl*II-*HOcs sam2*::*HIS3 HIS3*::*sam1*-Δ*5′*, Δ*Sal*I, *SSL1-3* pGHOT (*GAL*::*HO*, *TRP1*)

[a] All strains were originated in this study.

endonucleases that cut within the *RAD3* gene (39). The gapped plasmid was purified with gene clean (Bio 101, San Diego, Calif.) before transformation into a *rad3 ura3* mutant strain (50). Ura^+ transformants were assayed for the ability to grow at 37°C. The transformants that arose from the repair of plasmids that are missing a 502-bp *Cla*I-*Cla*I fragment always fail to grow at 37°C, mapping the mutation causing the Ts phenotype to this fragment. The *Cla*I-*Cla*I fragment recovered from the mutant by gap repair (57) was subcloned into pBluescript II SK+ and purified on Qiagen minicolumns (Diagen, Hilden, Germany). Sequencing revealed a single G-to-A transition at position 1783 (39), changing the amino acid at position 595 from a glycine to an arginine. All sequencing was performed with the Applied Biosystems automated DNA sequencer.

Recombination assays. (i) Spontaneous recombination. Spontaneous recombination rates were determined as previously described (6) with wild-type and *rad3-G595R* mutant cells containing a *sam1*-Δ*Bgl*II 4-bp insertion allele at the *SAM1* locus and a *sam2*-Δ*Sal*I 4-bp insertion allele at the *SAM2* locus. The median frequency was used to determine the rate by the method of Lea and Coulson (30). Statistical significance was determined by contingency χ^2 analysis with the Yates correction for continuity (9). All assays were conducted at 30°C.

(ii) Double-strand break-stimulated recombination. AdoMet auxotrophs are respiration-deficient cells (4) that cannot be grown on nonfermentable carbon sources (e.g., glycerol, lactate, and ethanol). Because of this, $AdoMet^-$ cells cannot be grown under conditions that neither induce nor repress the expression of the *GAL*::*HO* endonuclease fusion gene (25). As a result, we were unable to use methods, previously developed to measure double-strand break-stimulated recombination frequencies at the *MAT* locus (52), to measure double-strand break-stimulated recombination between the *SAM* genes.

To measure double-strand break-stimulated recombination frequencies between the *SAM* genes, we developed an assay that was derived from the replica-plating technique used to screen for elevated double-strand break-stimulated recombination among our Ts mutants. All of the strains that were assayed in this manner contain loss-of-function alleles at the *SAM1* and *SAM2* loci (Fig. 1) and require supplemental AdoMet (33 μg/ml) for growth. The strains were also maintained on medium lacking supplemental tryptophan to select for retention of the plasmid (pGHOT) containing the galactose-inducible HO endonuclease gene (25). Single colonies were dispersed in water with mild sonication. Then 50 to 100 CFU was plated onto 10 plates without Trp but with AdoMet and incubated at 23°C until the yeast colonies were 0.2 to 2 mm in diameter. The total number of colonies per plate was then determined. These colonies were replica plated onto plates without Trp but containing galactose (2%) and lacking supplemental AdoMet. These and the original plates (without Trp but with AdoMet) were incubated at 30°C for 5 to 7 days. Galactose induces expression of HO endonuclease from the *GAL*::*HO* fusion gene on pGHOT (25). The HO endonuclease cuts at its recognition sequence on a 117-bp fragment of the *MAT* locus (28, 41) embedded in one of the *SAM* genes (Fig. 1). The absence of AdoMet selects for cells in which a recombination event between the HO endonuclease-cut *SAM* gene and an unlinked *SAM* gene generates a functional *SAM* gene and an $AdoMet^+$ cell. The $AdoMet^+$ recombinants show up as papillae growing up out of a background of nongrowing cells. $AdoMet^+$ papillae arising on the original plate without Trp but with AdoMet also outgrow their $AdoMet^-$ progenitors. Colonies on the original plates that contain papillae are excluded from the frequency determination to prevent preexisting $AdoMet^+$ recombinant cells from affecting the calculations.

TABLE 2. Plasmids used in this study

Plasmid	Relevant gene	Description
pWJ425	*sam1*-Δ*Sal*I	1.7-kb *sam1*-Δ*Sal*I gene inserted downstream from *HIS3* coding sequence in *HIS3* genomic clone in pUC-HIS3
pWJ453	*sam2*-Δ*Sal*I	1.8-kb *sam2*-Δ*Sal*I gene inserted downstream from *HIS3* coding sequence in *HIS3* genomic clone in pUC-HIS3
pWJ457	*sam1*-Δ*Bgl*II-*HOcs*	117-bp HOcs fragment inserted into the *Bgl*II site in the *SAM1* coding sequence lying in the polylinker of pUC-URA3
pWJ493	*sam2*-Δ*Eco*RV-*HOcs*	117-bp HOcs fragment inserted into the *Eco*RV site in the *SAM2* coding sequence lying in the polylinker of pUC-URA3
pWJ542	*sam2*-Δ*Sal*I-*HOcs*	117-bp HOcs fragment inserted into the *Sal*I site in the *SAM2* coding sequence lying downstream from *HIS3* coding sequence in *HIS3* genomic clone in pUC-HIS3
pLAY73	*sam1*-Δ5′, Δ*Sal*I	1.4-kb *sam1*-Δ*Sal*I fragment extending from the second base pair of the initiation codon to the end of the gene inserted downstream from *HIS3* coding sequence in *HIS3* genomic clone in pUC-HIS3
pLAY77	*sam1*::*TRP1*	800-bp *TRP1* coding sequence replaces entire *SAM1* coding sequence in 1.7-kb *SAM1* genomic clone, leaving short 5′- and 3′-flanking *SAM1* genomic sequences.

Recombination frequencies were determined by a method that was inspired by but is distinct from the method for determining mutation rates described by Luria and Delbrück (32). The fraction of replicated colonies that did not give rise to recombinant papillae, the P_0 class of the Poisson distribution, was used to determine the average number of recombinants per colony (m) by the equation $m = -\ln P_0$. The average number of recombinants per colony (m) was then divided by the average number of viable cells in a replicated colony (n) to determine the recombination frequency. The number of viable cells in a typical colony replica (n) was determined by excising a piece of agar containing one colony replica from each replica plate immediately after replica plating, transferring it into 0.1 ml of water, vortexing, and determining the cell density by hemacytometer counts before plating appropriate dilutions on nonselective plates without Trp but with AdoMet. The number of colonies that arise after 5 to 7 days of growth at 30°C indicates how many viable cells were in the replica before any double-strand breaks were made. The recombination frequencies listed in Fig. 1 are the median values from at least 10 trials. Statistical significance was determined by contingency χ^2 analysis.

The DNA from selected AdoMet$^+$ recombinants arising from either spontaneous or double-strand break-stimulated recombination was obtained and subjected to genomic blot analysis as previously described (5, 6). Determining the nature of the event that resulted in AdoMet prototrophy requires digesting the DNA with enzymes that give diagnostic fragments if the insertions that inactivate the *SAM* genes are replaced with wild-type information (5, 6). Coconversion events are documented by digesting DNA from the recombinants with *Pvu*II before blotting and hybridization (Fig. 2).

(iii) Repair of double-strand breaks without homologous recombination. We measured the number of cells in a typical replica-plated colony to survive plating on galactose medium, because double-strand breaks can be healed at significant frequencies by mechanisms other than homologous recombination (29, 35). Aliquots of the same suspensions used to determine the number of viable cells in a replica-plated colony were plated on plates without Trp but with AdoMet and galactose and incubated at 30°C for 5 to 7 days. AdoMet is included in the medium because these double-strand break repair events would not be expected to generate an intact *SAM* gene. The frequency of double-strand break repair

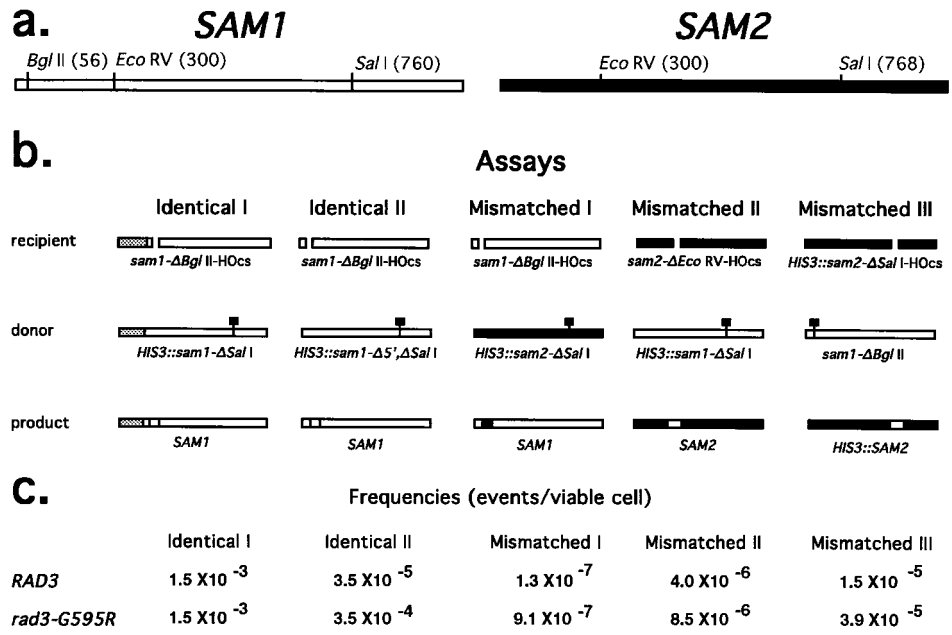

FIG. 1. Double-strand break-stimulated recombination frequencies. (a) *SAM1* and *SAM2* coding sequences, including relevant restriction sites. (b) Strains were built to measure the repair of a double-strand break by recombination. The double-strand breaks were created in either *SAM1* or *SAM2* coding sequences at one of three loci: the *SAM1* locus on chromosome XII, the *SAM2* locus on chromosome IV, or the *HIS3* locus on chromosome XV. The double-strand breaks (represented as gaps) were created by HO endonuclease within a 117-bp fragment of the *MAT* locus inserted into the *SAM1* or *SAM2* coding sequences that are the recipients of information from unlinked donor sequences. The unlinked donor sequences are defective *sam* genes that have been knocked out with 4-bp insertions (square flags). Only two genes can interact to give a wild-type *SAM* product by recombination, because either the *SAM1* or *SAM2* locus has a deletion/disruption allele. The *MAT* locus is also disrupted, restricting double-strand break formation to one site in the genome. (c) The assays were performed in isogenic wild-type and *rad3-G595R* mutant strains. Recombination frequencies were determined as described in the text. The median recombination frequency from at least 10 trials is reported. All assays were conducted at 30°C.

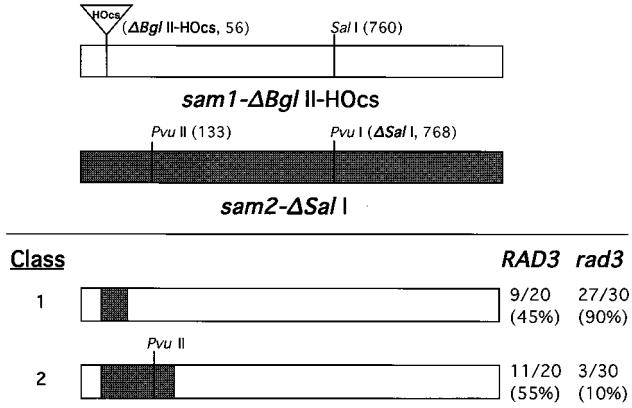

FIG. 2. Coconversion frequencies. Genomic DNA blots were performed to determine whether repair of a double-strand break at the *Bgl*II site of the *SAM1* gene by using *SAM2* sequences generated a *Pvu*II site 77 bp 3′ to the *Bgl*II site by coconversion. The parental *sam1*-Δ*Bgl*II-*HOcs* and *sam2*-Δ*Sal*I genes are depicted above the line. Depicted below the line are two different classes of *SAM1* recombinant. Class 1 recombinants have not incorporated the *Pvu*II site from the *sam2*-Δ*Sal*I gene during repair of the double-strand break at *SAM1*. Class 2 recombinants have incorporated the *Pvu*II site from the *sam2*-Δ*Sal*I gene. The fraction of the recombinants of each class obtained in a wild-type (*RAD3*) or *rad3-G595R* mutant background is reported. The corresponding percentages are listed in parentheses.

without homologous recombination was determined by dividing the number of survivors of plating on galactose medium by the number of viable cells plated. The median frequencies from 30 trials are reported.

(iv) Gene replacement. Homozygous wild-type or *rad3-G595R* mutant diploid strains that are homozygous for a null allele of *sam2* (*sam2*::*HIS3*), and heterozygous at the *SAM1* locus, having both a wild-type *SAM1* allele and a null *sam1*::*LEU2* allele, were constructed. These strains were transformed to tryptophan prototrophy with the *sam1*::*TRP1* fragment purified from an agarose gel with glass milk (Bio 101). The *sam1*::*TRP1* fragment has 42 bp at the 5′ end and 52 bp at the 3′ end that are homologous to 5′ and 3′ noncoding DNA flanking the *sam1*::*LEU2* target. Replacement of the *SAM1* allele is not observable, because loss of this allele renders the transformant unable to grow without supplemental AdoMet. Diploid strains were used in this analysis because the insertion of *sam1*::*TRP1* disrupts an upstream transcription unit that is essential for viability (4). Trp^+ transformants were replica plated to medium lacking leucine to screen for the loss of the *LEU2* marker. The DNA from several Leu^+ and Leu^- transformants was analyzed by genomic blotting.

Molecular analysis of double-strand break repair in wild-type and *rad3* mutant cells. (i) Time course. Molecular analysis of double-strand break repair was performed by a procedure similar to that described by Rudin and Haber (52). Wild-type and *rad3-G595R* $AdoMet^+$ cells containing an intact *SAM2* gene at the *HIS3* locus were used to inoculate 500 ml of medium (3% glycerol, 3% lactate) that neither induces nor represses expression of the *GAL*::*HO* gene, because $AdoMet^-$ cells cannot grow in this medium, as discussed above. The cultures were incubated at 30°C until they reached a density of 5×10^6 to 1.0×10^7 cells per ml as determined by counting with a hemacytometer. A 50-ml portion of cells were removed, counted with a hemacytometer, concentrated, and frozen. These cells were the −30-min time point. Then 50 ml of 20% galactose was added to the culture, which was incubated at 30°C. Another 50-ml aliquot of cells was removed after the 30-min incubation, counted, and processed as before. This was the 0-min time point. After removal of the 0-min aliquot the cells were filtered out of the galactose medium using a nitrocellulose filter apparatus (Nalgene). The filtrate was resuspended in glucose-containing medium that had been prewarmed to 30°C. Aliquots of cells were removed at 30-, 60-, or 120-min intervals, counted, and processed as before. Genomic DNA was prepared from the frozen cell pellets by the glass bead disruption method described by Hoffman and Winston (21).

(ii) Genomic blot analysis of time course DNA. A 1- to 2-μg portion of genomic DNA from each time point was digested with *Cla*I and *Sal*I, electrophoresed, and transferred to a positively charged nylon membrane (Hybond N+; Amersham) by using 0.4 N sodium hydroxide. The DNA on the blots was hybridized to a 460-bp *Eco*RV-*Sal*I fragment of the *SAM1* coding sequence (Fig. 1) labeled with ^{32}P by random priming (11). The information on the blot was revealed and quantitated either directly with a phosphorimager (Molecular Dynamics) or indirectly following autoradiography and quantitation with a densitometer (Molecular Dynamics).

(iii) Determination of single-stranded-DNA levels. A 1- to 2-μg portion of genomic DNA from each time point was transferred to a positively charged nylon membrane under either denaturing (0.4 N sodium hydroxide) or nondenaturing (3 M sodium chloride, 0.3 M sodium citrate [pH 7.0]) conditions by using a slot blot manifold (Bio-Rad). The DNA was fixed to the membrane with a UV cross-linker (Stratagene). The DNA on the blots was then hybridized with [^{32}P]RNA obtained by transcription of *SAM1* coding sequences from a plasmid containing a 704-bp *Bgl*II-*Sal*I DNA fragment of the *SAM1* gene (Fig. 1) linked to the SP6 and T7 promoters. Hybridization signals were quantitated with a phosphorimager.

(iv) Assay of recombinant product formation. A 1- to 2-μg portion of genomic DNA from each time point was used as a template for PCR detection of joint molecule formation between the HO endonuclease-cut fragment of chromosome XII carrying the 5′ end of the *sam1* gene and the *sam2* sequence at the *HIS3* locus (chromosome XV). The primers used were *SAM1*−366 (5′TACCGAA ACGGAGCTAAG3′), a sequence lying 366 bp 5′ to the beginning of the *SAM1* coding sequence, and *SAM2*74R (5′GGTCACAAATCTTGTCTG3′) a sequence lying 74 bp 3′ to the beginning of the *SAM2* coding sequence. The conditions for the PCR were one cycle of denaturation at 95°C for 5 min, annealing at 53°C for 2 min, and elongating at 72°C for 2 min, followed by 34 cycles of denaturation at 95°C for 1 min, annealing at 53°C for 1 min, and elongating at 72°C for 1 min. The PCR products were fractionated by electrophoresis on 1.2% agarose gels and were visualized by staining in 10 μg of ethidium bromide per ml before photography.

RESULTS

Recombination assays. We designed a series of genetic assays to study double-strand break-stimulated ectopic recombination in vegetative, haploid *S. cerevisiae* cells (Fig. 1). The *SAM1* and *SAM2* genes (83% identical at the DNA sequence level [64]), encoding AdoMet synthetase isozymes (64), were used in these assays. Homology between the *SAM1* and *SAM2* genes does not extend beyond their coding sequences (64). Duplicate *SAM1* genes were used to study recombination between sequences that share complete DNA sequence identity, while *SAM1* and *SAM2* genes were used to study recombination between mismatched sequences. A double-strand break in one of the *SAM* genes was created by HO endonuclease cutting at its recognition site (HO cut site) inserted at any of several positions in the coding sequence (see Materials and Methods). The double-strand break was repaired by using information donated by a second, unlinked *SAM* gene that was inactivated by a 4-bp insertion (6). Recombination between these sequences is restricted to nonreciprocal (gene conversion) and rare double-reciprocal events, because these genes have opposite orientations relative to their centromeres (4).

Double-strand breaks close to the edge of a gene are poor substrates for ectopic recombination. Double-strand breaks at the HO cut site in one *SAM* gene were readily healed by recombination with an unlinked *SAM* gene, because every $AdoMet^+$ recombinant analyzed by genomic blotting was missing the HO cut site (4). However, the efficiency of double-strand break repair was dependent on the position of the double-strand break relative to the border of homology between the two genes (Fig. 1). For example, *SAM1* × *SAM1* recombination occurred at a 43-fold-lower rate when a double-strand break near the border of the *SAM1* coding sequence was repaired by recombination with a duplicate *SAM1* sequence that has only 55 bp of DNA corresponding to one side of the break (Fig. 1, 3.5×10^{-5}, Identical II), than when the duplicate *SAM1* sequence has 279 bp of DNA corresponding to one side of the break (Fig. 1, 1.5×10^{-3}, Identical I). Additionally, recombination between the mismatched *SAM1* and *SAM2* genes (*SAM1* × *SAM2*) is 30- to 115-fold less efficient when double-strand breaks at the edge of the *SAM1* coding sequence are repaired with *SAM2* sequences (Fig. 1, 1.3×10^{-7}, Mismatched I) than when double-strand breaks at more centrally located sites in the *SAM2* gene (Fig. 1, 4.0×10^{-6}, Mismatched II, and 1.5×10^{-5}, Mismatched III) are repaired by recombination with *SAM1* sequences. Therefore, the length of homology shared between the ends of a double-strand break and an

unlinked duplicate sequence is an important determinant of how efficiently it is rescued by recombination.

Isolation of a Ts *rad3* mutant with elevated levels of double-strand break repair. We took a genetic approach to investigating the control of double-strand break-stimulated recombination between unlinked duplicate sequences. A wild-type strain containing one of the recombination assays described above (Table 1, Mismatched I) was mutagenized, and survivors were screened for temperature sensitivity and a hyperrecombination phenotype as described in Materials and Methods. The Ts mutant that consistently displayed the highest level of recombination was selected for further analysis. A diploid strain created by backcrossing the mutant with a wild-type strain neither was Ts nor showed elevated levels of recombination, indicating that both phenotypes are recessive. Tetrad analysis showed that the Ts and hyperrecombination phenotypes always cosegregated and were caused by a mutation in a single gene (4).

A genomic sequence that complemented the Ts phenotype of the mutant was obtained by selection following transformation with a yeast genomic library. A subclone that complemented the Ts growth and hyperrecombination phenotypes in the mutant strain was found to direct the integration of a plasmid to the Ts locus, since a *URA3* marker on the plasmid always segregated in repulsion with the Ts growth phenotype in crosses (4). This demonstrated that the wild-type allele of the Ts mutant gene had been cloned. This same subclone was also used as a hybridization probe of blots of both intact yeast chromosomes and restriction endonuclease-digested genomic DNA and revealed that the clone is a single-copy sequence that maps to chromosome V. When the 4.0-kb subclone was used to probe filters of arrayed λ clones of yeast genomic DNA, the positions corresponded to the *RAD3* locus on the right arm of chromosome V (49). The mutation in the *rad3* gene was mapped to a 502-bp *Cla*I-*Cla*I fragment of the *RAD3* coding sequence (39) by a standard gap repair protocol as described in Materials and Methods. The fragment carrying the mutation was sequenced, revealing a single G-to-A transition at nucleotide 1782 that changes glycine codon 595 to an arginine codon. This amino acid residue lies within the putative DNA-binding domain of the Rad3 helicase (15).

***rad3-G595R* stimulates the repair of a mutation lying at the edge of a gene by spontaneous ectopic recombination.** Elevated levels of spontaneous recombination have been observed previously in other *rad3* mutants (14, 37). We were interested in determining if the rate of spontaneous ectopic recombination was also elevated in *rad3-G595R* cells. Spontaneous recombination between the *SAM1* and *SAM2* genes at their native loci in *rad3-G595R* mutant cells was compared with recombination in wild-type cells. The *rad3-G595R* mutation led to a statistically significant increase ($P = 0.03$) in the repair of a 4-bp insertion 56 bp from the 5′ edge of the *SAM1* gene with respect to the repair of a 4-bp insertion at a more central location in the *SAM2* gene. Of 49 *rad3-G595R* recombinants, 14 were Sam1$^+$, while only 3 of 56 wild-type recombinants were Sam1$^+$. The overall rates of spontaneous recombination between the *SAM* genes in *rad3-G595R* (1.3×10^{-8}) and wild-type (9.1×10^{-9}) cells were not significantly different ($P = 0.27$), however.

***rad3-G595R* stimulates the repair of double-strand breaks that lie close to the edge of a gene.** The preferential repair of a mutation at the border of one gene by spontaneous recombination with an unlinked gene in *rad3-G595R* mutant cells led us to suspect that double-strand breaks near the edge of a gene might also be preferentially rescued by recombination in the *rad3-G595R* mutant. The rates of repair of double-strand breaks at different positions in the *SAM1* and *SAM2* genes by ectopic recombination were determined in *rad3-G595R* mutants and compared with the rates observed in wild-type cells (Fig. 1). The *SAM1* × *SAM2* recombination rate was 10-fold higher in *rad3-G595R* cells (3.4×10^{-4}) than in wild-type cells (3.5×10^{-5}) when a double-strand break at one end of *SAM1* was repaired by using a *SAM1* sequence that has only 55 bp of identical DNA sequence corresponding to one side of the break (Fig. 1, Identical II). Similarly, the *SAM1* × *SAM2* recombination rate was sevenfold higher in *rad3-G595R* mutant cells (9.1×10^{-7}) than in wild-type cells (1.3×10^{-7}) when a double-strand break at one edge of the *SAM1* gene was repaired by using mismatched *SAM2* gene sequences (Fig. 1, Mismatched I). This suggests that the *rad3-G595R* mutation stimulates the repair of double-strand breaks that lie near the edge of homology with their donor sequences.

Conversely, the repair of double-strand breaks that lie further from the border of homology with the donor sequence were less affected by the *rad3-G595R* mutation. The *SAM1* × *SAM1* recombination rate was the same in wild-type and *rad3-G595R* mutant cells (1.5×10^{-3}) when a double-strand break at one edge of the *SAM1* gene was repaired by using a *SAM1* sequence that has 279 bp of identical DNA sequence corresponding to one end of the break (Fig. 1, Identical I). In addition, the *SAM1* × *SAM2* recombination rate was not significantly increased in *rad3-G595R* mutant cells (Mismatched II, $P = 0.2$; Mismatched III, $P = 0.5$) when double-strand breaks at centrally located sites in the *SAM2* gene were repaired by using mismatched *SAM1* sequences (Fig. 1).

Because the frequencies of repair of double-strand breaks to give functional *SAM* genes were low (less than 0.2%) in all of our assays, we were eager to determine whether the frequency of all repair of double-strand breaks in the *sam* genes was low in our strains. To determine the overall level of survivorship of double-strand breaks, we determined the plating efficiency of cells containing an HO-cuttable *sam* allele and the galactose-inducible *HO* gene on galactose medium containing AdoMet. Interestingly, neither the position of the double-strand break nor the presence of the *rad3-G595R* mutation affected survival. A double-strand break at the 5′ end of the *SAM1* gene (Fig. 1, *Bgl*II site) resulted in a nearly identical frequency of survivors in wild-type cells (1.9×10^{-3}) and *rad3-G595R* cells (2.3×10^{-3}). Similarly, a double-strand break at a more central location in the *SAM2* gene (Fig. 1, *Eco*RV site) resulted in a frequency of survivors in wild-type cells (2.8×10^{-3}) that was very close to the frequency observed in *rad3-G595R* mutant cells (3.8×10^{-3}). Replica plating revealed that all of the survivors were AdoMet$^-$ cells, suggesting that the double-strand breaks may have been repaired by mechanisms other than homologous recombination (29, 35). To test this hypothesis, we measured the plating efficiency of cells on galactose plus AdoMet medium that contained an HO-cuttable *SAM1* allele (*sam1*-Δ*Bgl*II-*HOcs*) and the galactose-inducible *HO* gene but no other identical or mismatched *sam* sequences with which to repair the double-strand break by recombination. We found that survival in wild-type (1.9×10^{-3}) and *rad3-G595R* mutant (1.7×10^{-3}) cells was nearly identical to the survival observed when other *sam* information was present. These results suggest that the repair of double-strand breaks by mechanisms other than homologous recombination is position independent and occurs equally well in wild-type and *rad3-G595R* mutant cells. These results also indicate that fewer than 1% of the cells survive a double-strand break in a *SAM* gene.

***rad3-G595R* decreases coconversion of sequences flanking a double-strand break.** We reasoned that a mutation that selectively enhanced recombination between the sequences at the

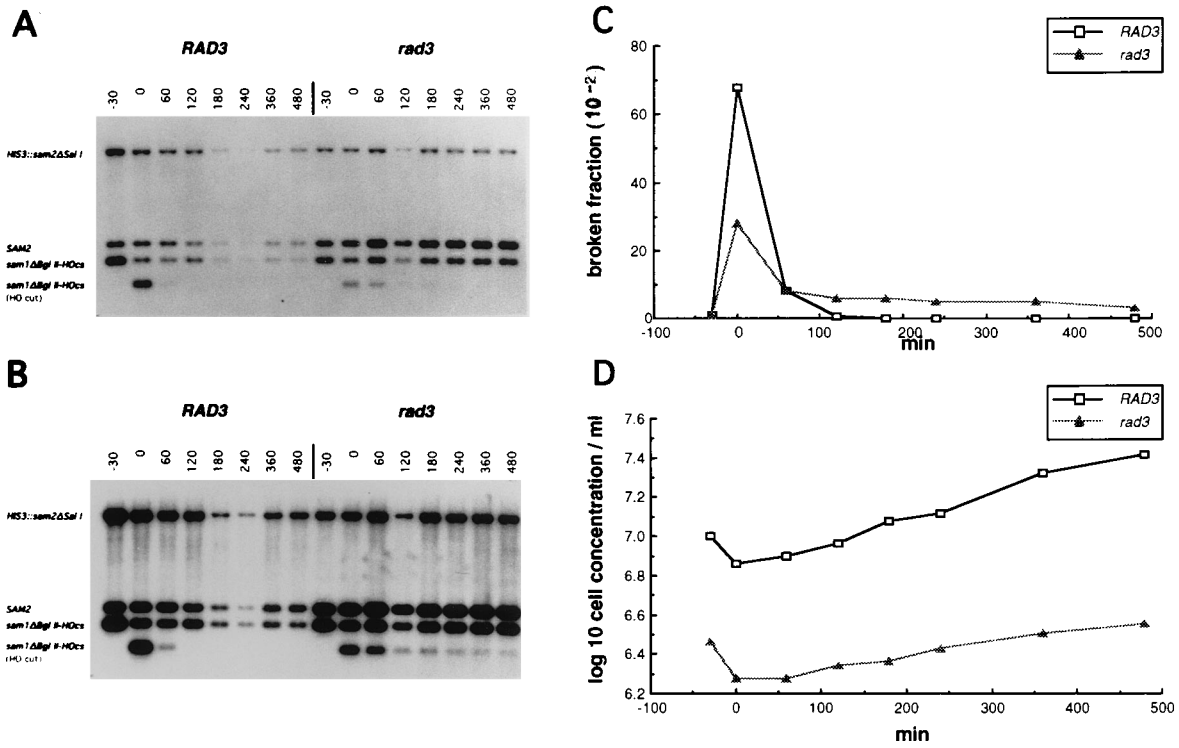

FIG. 3. Physical analysis of double-strand break repair in wild-type and *rad3-G595R* mutant cells. Genomic DNA was prepared from samples of wild-type and *rad3-G595R* cells collected from cultures at various times before and after double-strand breaks are created, as described in Materials and Methods. The DNA was digested with *Cla*I and *Sal*I, blotted, and hybridized with a radioactively labeled *SAM1* fragment, as described in Materials and Methods. The signals on these blots were visualized by autoradiography and measured by densitometry or measured directly with a phosphorimager. (A) A 14-h autoradiograph of genomic DNA from a time course study of the appearance and disappearance of HO-cut DNA. Signals corresponding to *HIS3*::*sam2*-Δ*Sal*I (7.6 kb), *SAM2* (1.2 kb), *sam1*-Δ*Bgl*II-*HOcs* (1,050 bp), and the *sam1*-Δ*Bgl*II-*HOcs* sequence cut with HO (770 bp) were visualized. There are two copies of the *SAM2* sequence in the *rad3-G595R* cells used in this analysis. This does not affect the results of the assay, because the same results were obtained when a single copy of the *SAM2* sequence was present in *rad3-G595R* cells (data not shown). (B) A 72-h autoradiograph of the same blot as in panel A. (C) Graph of the kinetics of the appearance and disappearance of HO-cut DNA. The level of HO-cut (broken) *sam1*-Δ*Bgl*II-*HOcs* signal as a fraction of the total *sam1*-Δ*Bgl*II-*HOcs* signal for each time point was determined by the formula [*sam1*-Δ*Bgl*II-*HOcs* (HO cut)]/{[*sam1*-Δ*Bgl*II-*HOcs* (HO cut)] + [*sam1*-Δ*Bgl*II-*HOcs*]}. (D) Graph of cell density during the time course. Cell density was determined by hemacytometer counts at every time point before the cells were collected for DNA preparation.

borders of duplicate genes might have affected the length of heteroduplex DNA that was formed between them. A conversion tract is the length of contiguous DNA sequence that has been gene converted, presumably by mismatch repair of the heteroduplex, and has previously been used as a gauge of the length of heteroduplex (27). Conversion tract length can be estimated by determining whether gene conversion has occurred at sites that flank the double-strand break. Genomic blots of DNA from recombinants (not shown) showed that the repair of a double-strand break at the *Bgl*II site of the *SAM1* gene by using *SAM2* sequences frequently resulted in the conversion of a sequence that lies 77 bp 3′ to the position of the break, resulting in the insertion of a *Pvu*II site (Fig. 2). This coconversion event (Fig. 2, class 2) occurred 55% (11 of 20) of the time in wild-type cells but only 10% (3 of 30) of the time in *rad3-G595R* mutant cells. This result suggests that while the frequency of recombination following a double-strand break at one end of *SAM1* by using *SAM2* sequences was increased in *rad3-G595R* mutant cells, heteroduplex DNA length was reduced.

Gene replacement with a selectable DNA fragment flanked with short sequences homologous to the *SAM1* locus is more efficient in *rad3-G595R* mutant cells. A mutation that enhanced the repair of a chromosomal double-strand break by using a short stretch of homology between donor and recipient might also be expected to permit a higher rate of recombination between an exogenous DNA fragment and the genome when short homologous sequences are used. We tested the efficiency of replacing a *LEU2* gene inserted within the *SAM1* coding sequence with an 800-bp clone of the *TRP1* coding sequence flanked by 42 bp of *SAM1* 5′ DNA and 52 bp of *SAM1* 3′ DNA in *rad3-G595R* mutant and wild-type cells (see Materials and Methods). Trp^+ transformants can be the result of either integration at the *SAM1* locus by using the *SAM1* ends or integration or gene conversion at the *TRP1* locus. Of 131 *rad3-G595R* Trp^+ transformants, 62 (47%) were the result of integration at the *SAM1* locus, while only 14 of 233 (6%) wild-type Trp^+ transformants were the result of recombination at *SAM1*. Genomic blots of several Trp^+ transformants revealed patterns that were consistent with the genetic results (4). These results indicate that the *rad3-G595R* allele increased the efficiency of integrating a DNA fragment into the genome by recombination between short terminal DNA sequences and homologous sequences in the genome.

Physical analysis of double-strand break repair in wild-type and *rad3-G595R* mutant cells. We conducted a physical analysis of double-strand break repair in *rad3-G595R* cells to search for the physical basis of the genetic results described above. We studied the repair of a double-strand break at one end of the *SAM1* gene by recombination with a mismatched *SAM2* donor sequence (Fig. 1, Mismatched I) at the DNA level. A brief period of expression of HO endonuclease created

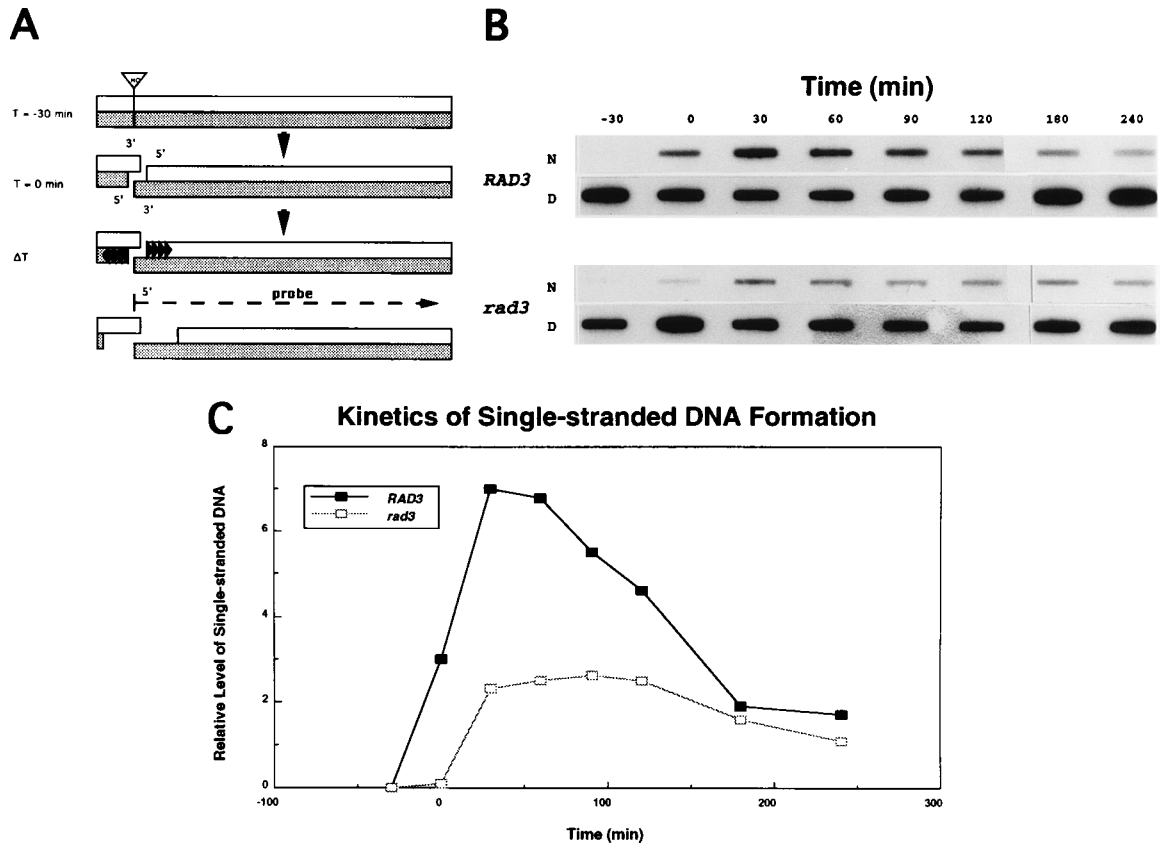

FIG. 4. Time course analysis of single-stranded DNA levels in wild-type and *rad3-G595R* mutant cells. (A) Cartoon of the assay. At the −30-min time point, the HO cut site (triangle) in *sam1-ΔBgl*II-*HOcs* is intact. Endonuclease cleavage at the HO cut site is allowed to occur for 30 min at 30°C ($T = 0$ min). The 5′ ends of the break are degraded over time (ΔT) by an unknown exonuclease (represented by solid black arrows pointing away from the break). Hybridization with a 704-bp ssRNA probe (described in Materials and Methods) reveals the amount of ssDNA formation. (B) Slot blots of native and denatured DNA from wild-type (*RAD3*) and mutant (*rad3*) cells. DNA prepared from the cells collected during the time course was transferred to nylon with a slot blot manifold under either nondenaturing (N) or denaturing (D) conditions, as described in Materials and Methods. The DNA was then hybridized with a 704-bp ssRNA probe, as described in Materials and Methods. The signals were visualized by autoradiography. The *rad3-G595R* cells used in this analysis had a single copy of the *SAM2* gene (see the legend to Fig. 3). (C) Graph picturing the kinetics of the appearance and disappearance of ssDNA. The signals obtained by hybridization were measured directly by phosphorimaging. The level of ssDNA at each time point was determined by dividing the signal from the nondenatured DNA (N in panel B) by the signal from the denatured DNA (D in panel B). These data were plotted against the time that the sample was collected.

a double-strand break at the *SAM1* locus in some fraction of the cells in a liquid culture. Genomic DNA was prepared from wild-type and *rad3-G595R* cells collected at intervals before and after the creation of the double-strand break. The DNA was then analyzed by genomic blotting and hybridization (Fig. 3A). Several differences between the wild-type and *rad3-G595R* DNAs were observed. Interestingly, just before the *GAL*::*HO* gene was turned off after 30 min of expression (0 min), a band corresponding to one end of the HO endonuclease-cut *SAM1* gene was more abundant in the wild-type cells than in the *rad3-G595R* mutant cells. Nearly 70% of the cells in the wild-type culture had cuts at the *SAM1* locus, while the *SAM1* locus had been cut in less than 30% of the *rad3-G595R* cells (Fig. 3C). The maximum levels of *SAM1* DNA cut by HO endonuclease during a 30-min period of induction in 10 independent trials were two- to threefold higher in wild-type cells (55 to 85% cut) than in *rad3-G595R* cells (25 to 45%) (4). From 60 to 90 min of induction was required to see 100% cutting in wild-type cells, while 120 to 180 min of induction was required to see 100% cutting in *rad3-G595R* mutant cells (4).

We have found that while the *SAM1* locus is cut more often in wild-type cells than in *rad3-G595R* cells, the broken DNA is more stable in *rad3-G595R* mutant cells. Genomic blots show that the original double-strand break signal is gone at the 180-min time point in wild-type cells, while the same signal persists until the end of the time course (480 min) in *rad3-G595R* mutant cells (Fig. 3B and C). The cell number remained nearly unchanged in both the wild-type and *rad3-G595R* cultures in the first 120 min following the end of *HO* gene expression (Fig. 3D), during which the original cut species nearly disappeared from the wild-type cells (Fig. 3B and C). This argues that the rapid kinetics of double-strand break signal loss in wild-type cultures could not be due to rapid growth of cells that contained uncut *SAM1* genes.

We further investigated the greater stability of double-strand breaks in *rad3-G595R* mutant cells by examining the kinetics of single-stranded DNA (ssDNA) formation and loss at the broken ends (Fig. 4). ssRNA probes (704 bp) complementary to opposite strands of the *SAM1* coding sequence immediately flanking one side of the double-strand break were used to determine the polarity and amount of double-strand break processing. Hybridization signals were obtained from slot blots of nondenatured DNA with the probe that is complementary to the 3′ strand (Fig. 4) but not the 5′ strand, indicating that double-strand break processing at the *SAM1* locus had the same polarity as at the *MAT* locus (71). Com-

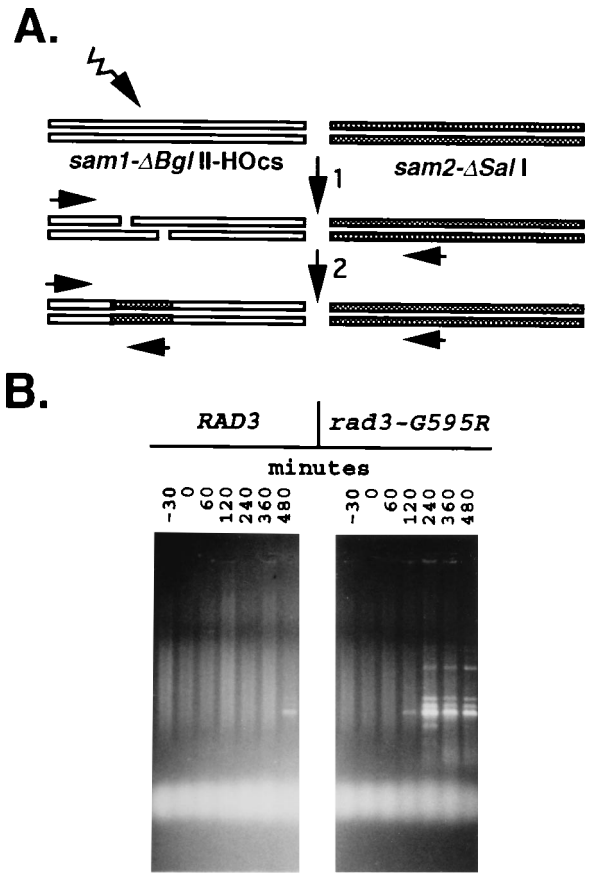

FIG. 5. Detection of recombination product by PCR. (A) Cartoon describing the strategy for detecting joint-molecule formation between *SAM1* and *SAM2* sequences following the creation of a double-strand break at the 5′ end of *SAM1* by PCR. 1. A double-strand break is created at the *Bgl*II site of the *sam1-ΔBgl*II-*HOcs* gene. Primers homologous to a sequence 366 bp 5′ to the start of the *SAM1* coding sequence on chromosome XII and 74 bp 3′ to the start of the *SAM2* coding sequence are unable to participate in the PCR before formation of joint molecules between *SAM1* and *SAM2* sequences. 2. Formation of a covalent linkage between the left side of the double-strand break at *SAM1* and *SAM2* sequences allows the primers to participate in a PCR that amplifies a 440-bp fragment corresponding to the distance between the primer-annealing sites on the recombination product. (B) DNA obtained from the wild-type and *rad3* mutant cells collected during the time course was subjected to PCR under the conditions described in Materials and Methods. The products were electrophoresed on agarose gels and were visualized by staining with ethidium bromide. The dominant species is approximately 440 bp in length and corresponds to the bona fide recombination product. The higher-molecular-weight species disappear at higher annealing temperatures, but the 440-bp band could not be visualized in the products of the PCR from wild-type DNA at those temperatures (data not shown).

paring the kinetics of ssDNA appearance and disappearance in *rad3-G595R* and wild-type cells showed that ssDNA was formed more slowly and disappeared more slowly in *rad3-G595R* cells than in wild-type cells (Fig. 4B and C). In wild-type cells, the maximum level of ssDNA was observed 30 min after HO gene expression ceased (30 min). Beyond that point, the level declined rapidly. The very low levels of double-strand break repair by homologous recombination (Fig. 1, Mismatched I) or other means (indicated by the low level of double-strand break repair without homologous recombination) suggest that the rapid disappearance of the ssDNA signal in wild-type cells (Fig. 4) is not due to the healing of the broken ends but instead is due to their degradation.

In contrast to observations with wild-type cells, we observed an initial delay in the formation of ssDNA in *rad3-G595R* cells, because signal levels were nearly undetectable at 0 min. Near-maximal levels of ssDNA were observed at the 30-min time point, and this level did not change significantly for another 90 min. The rate of decay of ssDNA after that point was lower than in wild-type cells. These results were very consistent throughout all 10 trials (4), indicating that the ends of a double-strand break are less susceptible to degradation in the *rad3-G595R* mutant cells.

The genetic results described above suggest that the repair of a double-strand break at one end of *SAM1* by recombination with *SAM2* occurs at a higher frequency in *rad3-G595R* cells than in wild-type cells. Using PCR, we detected covalent linkage between the end of the break at the *SAM1* gene with little homology to the *SAM2* gene and *SAM2* sequences at the 120-min time point in *rad3-G595R* cells, while we were unable to see any PCR product from wild-type DNA until the 480-min time point (Fig. 5). The delay in recombination in wild-type cells correlates with the rapid degradation of double-strand breaks (Fig. 3 and 4), suggesting perhaps that the end of the double-strand break with little homology with the donor is degraded past the point that it can efficiently recombine with donor sequences. The shorter sequences may require more attempts before recombination is successful, delaying recombinant product formation in wild-type cells. In contrast, the slower degradation of double-strand breaks in *rad3-G595R* mutant cells (Fig. 3) may allow the end of the break with little homology with the donor to retain a sufficient length of homology to more efficiently recombine with the donor sequence.

DISCUSSION

In this study, we examined the position dependence of the repair of a double-strand break in a gene by recombination with a second, unlinked copy of the gene and found that the frequency of recombination was much lower when the break was at the edge of homology between the two genes than when it was closer to the middle (Fig. 1). We also described a *rad3* mutant that exhibited increased levels of recombination between short homologous sequences while both repairing a double-strand break close to the edge of a gene (Fig. 1) and inserting an exogenous DNA fragment into the genome. Taken together, these results indicate that recombination between short homologous sequences is suppressed and that the *RAD3* gene is involved in that suppression in *S. cerevisiae.*

As discussed previously, the *RAD3* gene encodes a subunit of the transcription (10) and DNA repair (66) factor TFIIH. Consequently, a mutation in the *RAD3* gene could affect recombination by a variety of mechanisms. In fact, the codon altered by our *rad3* mutation (codon 595) is in a putative DNA-binding domain (15) and has previously been implicated in both the essential and DNA repair functions of *RAD3* (40). Likewise, our *rad3-G595R* allele appears to confer a gene expression defect, because the level of cutting by HO endonuclease obtained after a short period of *GAL*::*HO* gene expression in *rad3-G595R* mutant cells was about 40% of the level observed in wild-type cells (Fig. 3). Interestingly, we have found that a Ts allele (*SSL1-3*) of a gene that encodes another subunit of TFIIH (10) and confers a similar gene expression phenotype (73) does not confer an enhanced ability to use short homologous sequences for recombination (4). The different effects of the *rad3-G595R* and *SSL1-3* mutations on recombination suggest that the *RAD3* gene product could have separate roles in transcription and recombination.

Although the phenotypes of the *rad3-G595R* mutant suggest that the *RAD3* gene plays an important role in limiting recom-

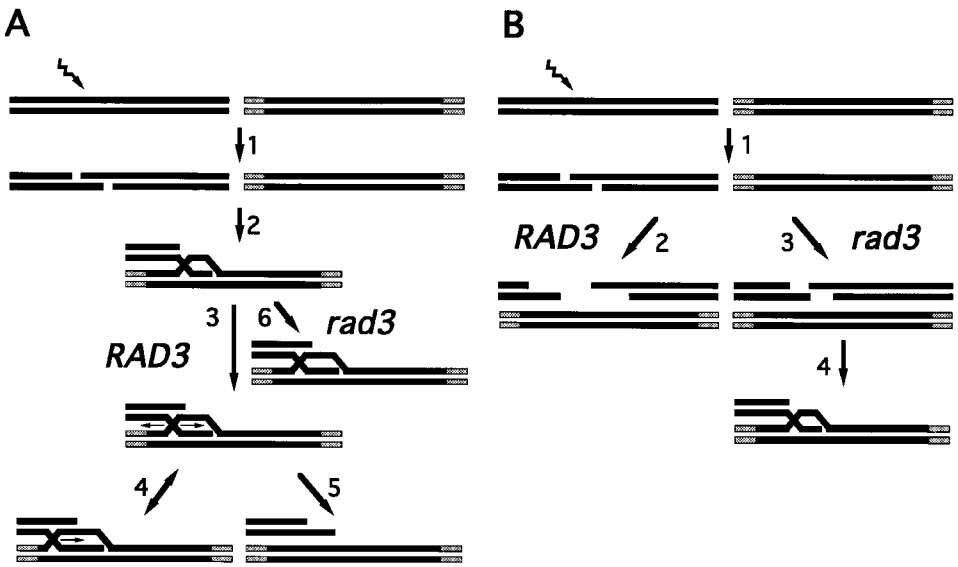

FIG. 6. Models describing how recombination between short homologous sequences may be restricted. (A) Branch migration model. A double-strand break at one edge of the coding sequence (step 1) creates ends that can invade an unlinked donor duplex (step 2). In wild-type (*RAD3*) cells, movement of the Holliday junction or branch migration enlarges the tract of heteroduplex linking the donor and recipient duplexes (step 3). The extent of branch migration on the left side of the break is restricted, however, because that end is very close to the end of homology between the donor duplex and the invading end of the double-strand break. Once the Holliday junction stops at the homology boundary, reverse branch migration (step 4) could readily dissolve the short tract of heteroduplex (step 5), aborting recombination. In contrast, a reduced level of forward and reverse branch migration in *rad3-G595R* mutant cells (step 6) would stabilize the association between the donor and the recipient. The rescue of the other end of the double-strand break from the same donor duplex is not pictured but would be required to obtain a viable product of double-strand break repair. (B) Degradation model. Following the creation of a double-strand break at one edge of the coding sequence (step 1), degradation of the ends occurs. Digestion of the 5′ ends occurs first, leading to the creation of 3′ single strands, but physical evidence (see the text) suggests that the 3′ single strands are also degraded if the breaks are not repaired (Fig. 4). Degradation of both the 5′ and 3′ ends appears to be more rapid in wild-type (*RAD3*) cells (step 2) than in *rad3-G595R* mutant cells (step 3). Rapid degradation in wild-type cells may leave insufficient homology for pairing, strand invasion, or any homology-dependent step in recombination to occur efficiently between the left end of the break at *SAM1* and the unlinked *SAM2* donor. Conversely, the slow degradation of the ends of the break observed in *rad3-G595R* mutant cells (Fig. 4 and 5) may leave sufficient homology to repair the left end of the break more efficiently (step 4). Not pictured is the invasion of the donor duplex by the right side of the break that must occur before recombination can be completed.

bination between short DNA sequences, no direct role for Rad3 in recombination has yet been demonstrated. Consequently, we will consider both direct and indirect roles for Rad3 in the following models for restricting recombination between short sequences. The first model suggests that recombination between short homologous sequences may be regulated by the opposing forces of branch migration and reverse branch migration (Fig. 6A). Branch migration is the exchange of DNA strands between recombination partners that occurs when the Holliday junction, the recombination intermediate that ties the donor and recipient together (22), moves along the DNA. When donor and recipient share only short lengths of homology, branch migration cannot create long tracts of heteroduplex DNA. Reverse branch migration can easily dissolve short tracts of heteroduplex, aborting recombination.

Rad3p might function like the bacterial helicase RuvAB (69), which, like Rad3 (17), has been shown to have 5′-to-3′ strand displacement activity (65) but has also been shown to promote branch migration (38, 55). If Rad3 promotes branch migration in *S. cerevisiae*, it could drive the synthesis of heteroduplex DNA between the broken recipient and intact donor sequences. Mismatch repair of the heteroduplex DNA could explain the coconversion (Fig. 2) observed flanking the double-strand break (33, 44). Rad3 might also stimulate a yeast reverse branch migration factor, like the *E. coli* helicase RecG (31, 70), that could dissolve heteroduplex DNA and abort recombination. If *rad3-G595R* cells are helicase defective, branch migration and reverse branch migration would be affected. A decrease in branch migration would reduce heteroduplex length and the incidence of coconversion, while a decrease in reverse branch migration would increase heteroduplex stability and the frequency of recombination between short homologous sequences. Alternatively, Rad3p could have an indirect role in this model by modulating the expression of the genes encoding the branch migration, reverse branch migration, and mismatch repair activities.

The second model suggests that recombination between short homologous sequences (Fig. 6B) is restricted by degradation of the ends of broken DNA molecules. The ends might not have to be completely removed if shortening the sequence to any degree significantly reduces the efficiency of the recombination that follows. In fact, the 56 bp of homology between one end of the double-strand break at the *SAM1* gene and the unlinked *SAM2* donor sequences (Fig. 1, Mismatched I) already lies below the minimum length of DNA required for efficient recombination in yeast cells (2, 26, 58), arguing that even a modest loss of sequence length could significantly reduce the recombination rate. The physical data indicate that both the 5′ and 3′ strands of the double-strand break are more stable in the *rad3-G595R* mutant (Fig. 5), suggesting that perhaps the *RAD3* gene is involved in restricting recombination between short DNA sequences by increasing the degradation of broken DNA molecules. A decreased incidence of coconversion in *rad3-G595R* mutant cells (Fig. 2) is consistent with *RAD3* having a role in the creation of heteroduplex, possibly by increasing the length of 3′ single strands through promotion of degradation of the 5′ ends.

Rad3 helicase may promote the degradation of broken DNA by opening up the ends of the duplex to nucleases, as has been suggested previously (1). The requirement for a 3′ single strand demonstrated by Rad3p in vitro (17, 61) suggests that some exo- or endonucleolytic processing might be required

before Rad3p could act. Alternatively, Rad3p could act as part of an ensemble of proteins, such as the multifunctional assembly TFIIH (10, 66), opening DNA by an as yet uncharacterized mechanism. If Rad3p acts indirectly, it could regulate the expression of a wide array of genes encoding DNA-processing enzymes that degrade the ends of broken DNA.

The recombination phenotypes of the *rad3-G595R* mutant suggest a role for *RAD3* in maintaining genome stability in *S. cerevisiae*. The preferential stimulation of the repair of a mutation near the edge of a gene by spontaneous ectopic recombination in the *rad3-G595R* mutant suggests that *RAD3* should most strongly affect recombination between short repeated sequences, because a recombinogenic lesion in a short sequence is near to the edge of the sequence, even if it is at its center. Therefore, *RAD3* may be involved in determining the minimum DNA sequence length (26) required for efficient spontaneous recombination between dispersed repeated sequences. Interestingly, the minimum DNA sequence lengths for recombination in yeast cells and mammalian cells are very similar (≈250 bp [26, 51]). One intriguing speculation is that *RAD3* and its mammalian homolog *XPD* (60, 67) are both involved in the maintenance of genome integrity. This would give further support to previous observations (56) that, like several other DNA repair pathways (12, 68), recombination is conserved in *S. cerevisiae* and humans.

ACKNOWLEDGMENTS

We thank A. Wu, R. J. Lin, J. Termini, S. Gangloff, J. Smith, H. Zhou, and N. Erdeniz and several anonymous reviewers for helpful comments on the manuscript. Thanks are due to R. Rothstein and L. Symington for helpful discussions. We also thank T. Donahue, J. Haber, R. Kostricken, R. Jensen, and I. Herskowitz for plasmids used during this project. We thank R. Rothstein for support during the initial phases of this project.

This work was supported by the NCI (CA33572) as well as funds from the City of Hope and the Beckman Research Institute.

REFERENCES

1. **Aguilera, A., and H. L. Klein.** 1989. Yeast intrachromosomal recombination: long gene conversion tracts are preferentially associated with reciprocal exchange and require the *RAD1* and *RAD3* gene products. Genetics **123:** 683–694.
2. **Ahn, B.-Y., and D. Livingston.** 1986. Mitotic gene conversion lengths, coconversion patterns, and the incidence of reciprocal recombination in a *Saccharomyces cerevisiae* plasmid system. Mol. Cell. Biol. **6:**3685–3693.
3. **Alani, E., R. Padmore, and N. Kleckner.** 1990. Analysis of wild-type and *rad50* mutants of yeast suggests an intimate relationship between meiotic chromosome synapsis and recombination. Cell **61:**419–436.
4. **Bailis, A. M.** Unpublished observations.
5. **Bailis, A. M., L. Arthur, and R. Rothstein.** 1992. Genome rearrangement in *top3* mutants of *Saccharomyces cerevisiae* requires a functional *RAD1* excision repair gene. Mol. Cell. Biol. **12:**4988–4993.
6. **Bailis, A. M., and R. Rothstein.** 1990. A defect in mismatch repair in *Saccharomyces cerevisiae* stimulates ectopic recombination between homeologous genes by an excision repair dependent process. Genetics **126:**535–547.
7. **Cao, L., E. Alani, and N. Kleckner.** 1990. A pathway for generation and processing of double-strand breaks during meiotic recombination in *Saccharomyces cerevisiae*. Cell **61:**1089–1102.
8. **Christiansen, T. W., R. S. Sikorski, M. Dante, J. H. Shero, and P. Hieter.** 1991. Multifunctional yeast high-copy number shuttle vectors. Gene **110:**119–122.
9. **Cochran, W. G.** 1954. Some methods for strengthening the common chi-square tests. Biometrics **10:**417–427.
10. **Feaver, W. J., J. Q. Svejstrup, L. Bardwell, A. J. Bardwell, A. Buratowski, K. D. Gulyas, T. F. Donahue, E. C. Friedberg, and R. D. Kornberg.** 1993. Dual roles of a multiprotein complex from *Saccharomyces cerevisiae* in transcription and DNA repair. Cell **75:**1379–1387.
11. **Feinberg, A. P., and B. Vogelstein.** 1984. A technique for radiolabelling DNA restriction endonuclease fragments to high specific activity. Anal. Biochem. **137:**266–267.
12. **Fishel, R., M. K. Lescoe, M. R. S. Rao, N. G. Copeland, N. A. Jenkins, J. Garber, M. Kane, and R. Kolodner.** 1993. The human mutator gene homolog *MSH2* and its association with hereditary nonpolyposis colon cancer. Cell **75:**1027–1038.
13. **Friedberg, E. C., W. Siede, and A. J. Cooper.** 1991. Cellular responses to DNA damage in yeast, p. 147–192. *In* J. R. Broach, J. R. Pringle, and E. W. Jones (ed.), The molecular and cellular biology of the yeast *Saccharomyces*: genome dynamics, protein synthesis and energetics. Cold Spring Harbor Laboratory Press, Cold Spring Harbor, N.Y.
14. **Golin, J. E., and M. S. Esposito.** 1977. Evidence for joint genic control of spontaneous mutation and genetic recombination during mitosis in Saccharomyces. Mol. Gen. Genet. **150:**127–135.
15. **Gorbalenya, A. E., E. V. Koonin, A. P. Donchenko, and V. M. Blinov.** 1989. Two related superfamilies of putative helicases involved in replication, recombination, repair and expression of DNA and RNA genomes. Nucleic Acids Res. **17:**4713–4730.
16. **Guzder, S. N., H. Qiu, C. H. Sommers, P. Sung, L. Prakash, and S. Prakash.** 1994. DNA repair gene *RAD3* of *Saccharomyces cerevisiae* is essential for transcription by RNA polymerase II. Nature (London) **367:**91–94.
17. **Harosh, I., L. Naumovski, and E. C. Friedberg.** 1989. Purification and characterization of the Rad3 ATPase/DNA helicase from *Saccharomyces cerevisiae*. J. Biol. Chem. **264:**20532–20539.
18. **Harris, S., K. S. Rudnicki, and J. E. Haber.** 1994. Gene conversions and crossing over during homologous and homeologous ectopic recombination in *Saccharomyces cerevisiae*. Genetics **135:**5–16.
19. **Hinnen, A., J. B. Hicks, and G. R. Fink.** 1978. Transformation of yeast. Proc. Natl. Acad. Sci. USA **75:**1929–1933.
20. **Hobbs, H., M. Brown, J. Goldstein, and D. Russell.** 1986. Deletion of exon encoding cysteine-rich repeat of low density lipoprotein receptor alters its binding specificity in a subject with familial hypercholesterolemia. J. Biol. Chem. **261:**13114–13120.
21. **Hoffman, C. S., and F. Winston.** 1987. A ten-minute DNA preparation efficiently releases autonomous plasmids for transformation of *Escherichia coli.* Gene **94:**267–272.
22. **Holliday, R.** 1964. A mechanism for gene conversion in fungi. Genet. Res. **5:**292–304.
23. **Ito, H., Y. Fukuda, K. Murata, and A. Kimura.** 1983. Transfomation of intact yeast cells treated with alkali cations. J. Bacteriol. **153:**163–168.
24. **Jagadeeswaran, P., D. Tuan, B. G. Forget, and S. M. Weissman.** 1982. A gene deletion ending at the mid-point of a repetitive DNA sequence in one form of hereditary persistence of fetal hemoglobin. Nature (London) **296:** 469–470.
25. **Jensen, R. E., and I. Herskowitz.** 1984. Directionality and regulation of cassette substitution in yeast. Cold Spring Harbor Symp. Quant. Biol. **49:** 97–104.
26. **Jinks-Robertson, S., M. Michelitch, and S. Ramcharan.** 1993. Substrate length requirements for efficient mitotic recombination in *Saccharomyces cerevisiae*. Mol. Cell. Biol. **13:**3937–3950.
27. **Judd, S. R., and T. D. Petes.** 1988. Physical lengths of meiotic and mitotic gene conversion tracts in *Saccharomyces cerevisiae*. Genetics **118:**401–414.
28. **Kostricken, R., J. N. Strathern, A. J. S. Klar, J. B. Hicks, and F. Heffron.** 1983. A site-specific endonuclease essential for mating-type switching in *Saccharomyces cerevisiae*. Cell **35:**167–174.
29. **Kramer, K. M., J. A. Brock, K. Bloom, J. K. Moore, and J. E. Haber.** 1994. Two different types of double-strand breaks in *Saccharomyces cerevisiae* are repaired by similar *RAD52*-independent, nonhomologous recombination events. Mol. Cell. Biol. **14:**1293–1301.
30. **Lea, D. E., and C. A. Coulson.** 1949. The distribution of the numbers of mutants in bacterial populations. J. Genet. **49:**264–284.
31. **Lloyd, R. G., and G. J. Sharples.** 1993. Processing of recombination intermediates by the RecG and RuvAB proteins of *Escherichia coli*. Nucleic Acids Res. **21:**1719–1725.
32. **Luria, S. E., and M. E. Delbrück.** 1943. Mutations of bacteria from virus sensitivity to virus resistance. Genetics **28:**491–511.
33. **McGill, C., B. Shafer, and J. N. Strathern.** 1989. Co-conversion of flanking sequences with homothallic switching. Cell **57:**459–467.
34. **Meselson, M., and C. M. Radding.** 1975. A general model for genetic recombination. Proc. Natl. Acad. Sci. USA **72:**358–361.
35. **Mezard, C., and A. Nicolas.** 1994. Homologous, homeologous, and illegitimate repair of double-strand breaks during transformation of a wild-type strain and a *rad52* mutant strain of *Saccharomyces cerevisiae*. Mol. Cell. Biol. **14:**1278–1292.
36. **Mezard, C., D. Pompon, and A. Nicolas.** 1992. Recombination between similar but not identical DNA sequences during yeast transformation occurs within short stretches of identity. Cell **70:**659–670.
37. **Montelone, B. A., M. E. Hoekstra, and R. E. Malone.** 1988. Spontaneous mitotic recombination in yeast: the hyper-recombinational rem1 mutations are alleles of the *RAD3* gene. Genetics **119:**289–301.
38. **Müller, B., I. Tsaneva, and S. C. West.** 1993. Branch migration of Holliday junctions promoted by the *Escherichia coli* RuvA and RuvB proteins. I. Comparison of the RuvAB and RuvB mediated reactions. J. Biol. Chem. **268:**17185–17189.
39. **Naumovski, L., G. Chu, P. Berg, and E. C. Friedberg.** 1985. *RAD3* gene of *Saccharomyces cerevisiae*: nucleotide sequence of wild-type and mutant alleles, transcript mapping, and aspects of gene regulation. Mol. Cell. Biol. **5:**17–26.

40. **Naumovski, L., and E. C. Friedberg.** 1986. Analysis of the essential and excision repair functions of the *RAD3* gene of *Saccharomyces cerevisiae* by mutagenesis. Mol. Cell. Biol. **6:**1218–1227.
41. **Nickoloff, J., E. Y. Chen, and F. Heffron.** 1986. A 24-base-pair DNA sequence from the *MAT* locus stimulates intergenic recombination in yeast. Proc. Natl. Acad. Sci. USA **83:**7831–7835.
42. **Petes, T. D., and C. W. Hill.** 1988. Recombination between repeated sequences in microorganisms. Annu. Rev. Genet. **22:**147–168.
43. **Priebe, S. D., J. Westmoreland, T. Nilsson-Tillgren, and M. A. Resnick.** 1994. Induction of recombination between homologous and diverged DNAs by double-strand gaps and breaks and role of mismatch repair. Mol. Cell. Biol. **14:**4802–4814.
44. **Ray, B. L., C. I. White, and J. E. Haber.** 1991. Heteroduplex formation and mismatch repair of the "stuck" mutation during mating-type switching in *Saccharomyces cerevisiae*. Mol. Cell. Biol. **11:**5372–5380.
45. **Rayssiguier, C., D. S. Thaler, and M. Radman.** 1989. The barrier to recombination between *Escherichia coli* and *Salmonella typhimurium* is disrupted in mismatch-repair mutants. Nature (London) **342:**396–400.
46. **Resnick, M. A.** 1976. The repair of double-strand breaks in DNA: a model involving recombination. J. Theor. Biol. **59:**97–106.
47. **Resnick, M. A., M. Skaanild, and T. Nilsson-Tillgren.** 1989. Lack of DNA homology in a pair of divergent chromosomes greatly sensitizes them to loss by DNA damage. Proc. Natl. Acad. Sci. USA **86:**2276–2281.
48. **Reynolds, R. J., and E. C. Friedberg.** 1981. Molecular mechanisms of pyrimidine dimer excision in *Saccharomyces cerevisiae*: incision of ultraviolet-irradiated deoxyribonucleic acid in vivo. J. Bacteriol. **146:**692–704.
49. **Riles, L., J. E. Dutchik, B. K. McCauley, E. C. Thayer, M. P. Leckie, V. V. Braden, J. E. Depke, and M. V. Olson.** 1993. Physical maps of the six smallest chromosomes of *Saccharomyces cerevisiae* at a resolution of 2.6 kilobase pairs. Genetics **134:**81–150.
50. **Rothstein, R.** 1991. Targeting, disruption, replacement, and allele rescue: integrative DNA transformation in yeast. Methods Enzymol. **194:**281–301.
51. **Rubnitz, J., and S. Subramani.** 1984. The minimum amount of homology required for homologous recombination in mammalian cells. Mol. Cell. Biol. **4:**2253–2258.
52. **Rudin, N., and J. E. Haber.** 1988. Efficient repair of HO-induced chromosomal breaks in *Saccharomyces cerevisiae* by recombination between flanking homologous sequences. Mol. Cell. Biol. **8:**3918–3928.
53. **Shen, P., and H. V. Huang.** 1986. Homologous recombination in *Escherichia coli*: dependence on substrate length and homology. Genetics **112:**441–457.
54. **Sherman, F., G. R. Fink, and J. B. Hicks.** 1986. Methods in yeast genetics. Cold Spring Harbor Laboratory Press, Cold Spring Harbor, N.Y.
55. **Shiba, T., H. Iwasaki, A. Nakata, and H. Shinagawa.** 1991. SOS-inducible DNA repair proteins, RuvA and RuvB, of *Escherichia coli*: functional interactions between RuvA and RuvB for ATP hydrolysis and renaturation of the cruciform structure in supercoiled DNA. Proc. Natl. Acad. Sci. USA **88:**8445–8449.
56. **Shinohara, A., H. Ogawa, Y. Matsuda, N. Ushio, K. Ikeo, and T. Ogawa.** 1993. Cloning of human, mouse and fission yeast recombination genes homologous to *RAD51* and *recA*. Nat. Genet. **4:**239–243.
57. **Strathern, J. N., and D. R. Higgins.** 1991. Recovery of plasmids from yeast into *Escherichia coli*: shuttle vectors. Methods Enzymol. **194:**319–328.
58. **Sugawara, N., and J. E. Haber.** 1992. Characterization of double-strand break induced recombination: homology requirements and single-stranded DNA formation. Mol. Cell. Biol. **12:**563–575.
59. **Sun, H., D. Treco, and J. Szostak.** 1991. Extensive 3′-overhanging, single-stranded DNA associated with the meiosis specific double-strand breaks at the *ARG4* recombination initiation site. Cell **64:**1155–1161.
60. **Sung, P., V. Bailly, C. Weber, L. H. Thompson, L. Prakash, and S. Prakash.** 1993. Human xeroderma pigmentosum group D gene encodes a DNA helicase. Nature (London) **365:**852–855.
61. **Sung, P., L. Prakash, S. W. Matson, and S. Prakash.** 1987. *RAD3* protein of *Saccharomyces cerevisiae* is a DNA helicase. Proc. Natl. Acad. Sci. USA **84:**8951–8955.
62. **Szostak, J. W., T. L. Orr-Weaver, R. Rothstein, and F. W. Stahl.** 1983. The double strand-break model for recombination. Cell **33:**25–35.
63. **Thomas, B. J., and R. Rothstein.** 1989. The genetic control of direct-repeat recombination in *Saccharomyces*: the effect of *rad52* and *rad1* on mitotic recombination at *GAL10*, a transcriptionally regulated gene. Genetics **123:**725–738.
64. **Thomas, D., R. J. Rothstein, N. Rosenberg, and Y. Surdin-Kerjan.** 1988. *SAM2* encodes the second methionine *S*-adenosyl transferase in *Saccharomyces cerevisiae*: physiology and regulation of both enzymes. Mol. Cell. Biol. **8:**5132–5139.
65. **Tsaneva, I. R., B. Müller, and S. C. West.** 1993. The RuvA and RuvB proteins of *E. coli* exhibit DNA helicase activity *in vitro*. Proc. Natl. Acad. Sci. USA **90:**1315–1319.
66. **Wang, Z., J. Q. Svejstrup, W. J. Feaver, X. Wu, R. D. Kornberg, and E. C. Friedberg.** 1994. Transcription factor b (TFIIH) is required during nucleotide excision repair in yeast. Nature (London) **368:**74–76.
67. **Weber, C. A., E. P. Salazar, S. A. Stewart, and L. H. Thompson.** 1990. *ERCC2*: cDNA cloning and molecular characterization of a human nucleotide excision repair gene with high homology to yeast *RAD3*. EMBO J. **9:**1437–1447.
68. **Weeda, G., J. H. J. Hoeijmakers, and D. Bootsma.** 1993. Genes controlling nucleotide excision repair in eukaryotic cells. Bioessays **15:**249–258.
69. **West, S. C.** 1994. The processing of recombination intermediates: mechanistic insights from studies of bacterial proteins. Cell **76:**9–15.
70. **Whitby, M. C., L. Ryder, and R. G. Lloyd.** 1993. Reverse branch migration of Holliday junctions by RecG protein: a new mechanism for resolution of intermediates in recombination and DNA repair. Cell **75:**341–350.
71. **White, C. I., and J. E. Haber.** 1990. Intermediates of recombination during mating type switching in *Saccharomyces cerevisiae*. EMBO J. **9:**663–673.
72. **Wilcox, D. R., and L. Prakash.** 1981. Incision and postincision step of pyrimidine dimer removal in excision-defective mutants of *Saccharomyces cerevisiae*. J. Bacteriol. **148:**618–623.
73. **Yoon, H., S. P. Miller, E. K. Pabich, and T. F. Donahue.** 1993. *SSL1*, a suppressor of a *HIS4* 5′-UTR stem-loop mutation, is essential for translation initiation and affects UV resistance in yeast. Genes Dev. **6:**2463–2477.